ACCOUNTS of chemical research

Article

pubs.acs.org/accounts

Self-Assembly of Intramolecular Charge-Transfer Compounds into Functional Molecular Systems

Yongjun Li, Taifeng Liu, Huibiao Liu,* Mao-Zhong Tian, and Yuliang Li*

Beijing National Laboratory for Molecular Sciences (BNLMS), CAS Key Laboratory of Organic Solids, Institute of Chemistry, Chinese Academy of Sciences, Beijing 100190, P.R. China

CONSPECTUS: Highly polarized compounds exhibiting intramolecular charge transfer (ICT) are used widely as nonlinear optical (NLO) materials and red emitters and in organic light emitting diodes. Low-molecular-weight donor/acceptor (D/A)-substituted ICT compounds are ideal candidates for use as the building blocks of hierarchically structured, multifunctional self-assembled supramolecular systems. This Account describes our recent studies into the development of functional molecular systems with well-defined self-assembled structures based on charge-transfer (CT) interactions. From solution (sensors) to the solid state (assembled structures), we have fully utilized intrinsic and stimulus-induced CT interactions to construct these functional molecular systems.

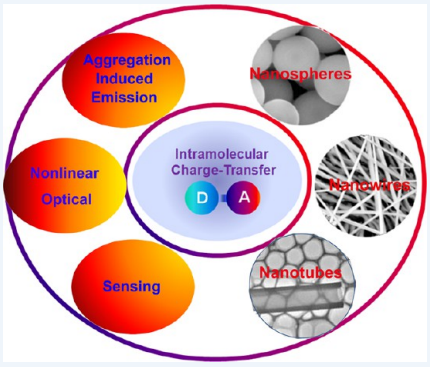

We have designed some organic molecules capable of ICT, with diversity and tailorability, that can be used to develop novel self-assembled materials. These ICT organic molecules are based on a variety of simple structures such as perylene bisimide, benzothiadiazole, tetracyanobutadiene, fluorenone, isoxazolone, BODIPY, and their derivatives. The degree of ICT is influenced by the nature of both the bridge and the substituents. We have developed new methods to synthesize ICT compounds through the introduction of heterocycles or heteroatoms to the π-conjugated systems or through extending the conjugation of diverse aromatic systems via another aromatic ring.

Combining these ICT compounds featuring different D/A units and different degrees of conjugation with phase transfer methodologies and solvent-vapor techniques, we have self-assembled various organic nanostructures, including hollow nanospheres, wires, tubes, and ribbonlike architectures, with controllable morphologies and sizes. For example, we obtained a noncentrosymmetric microfiber structure that possessed a permanent dipole along its fibers' long axis and a transition dipole perpendicular to it; the independent NLO responses of this material can be separated and tuned spectroscopically and spatially. The ready processability and intrinsically high NLO efficiency of these microfibers offer great opportunities for applications in photonic devices. We have also designed molecular sensors based on changes in the efficiency of the ICT process upon complexation of an analyte with the D or A moieties in the ICT compounds. Such sensors, which display evident Stokes shifts or changes in quantum yields or fluorescence lifetimes, have promise for applications in chemical and biological recognition and sensing.

In this Account, we shed light on the structure–function relationships of these functional molecular systems with well-defined self-assembled structures based on ICT interactions. The encouraging results that we have obtained suggest that such self-assembled ICT molecular materials can guide the design of new nanostructures and materials from organic systems, and that these materials, across a range of compositions, sizes, shapes, and functionalities, can potentially be applied in the fields of electronics, optics, and optoelectronics.

1. INTRODUCTION

Because of their potential applications in diverse fields (e.g., molecular electronics, light–energy conversion, catalysis, sensors), organic functional molecular systems with well-defined structures and morphologies have attracted great attention in recent years.[1,2] Intermolecular interactions, most commonly hydrogen bonding, π–π, and electrostatic interactions, can be used to tune the factors influencing the self-assembly and final morphologies of these systems; liquid–liquid or liquid–solid interfaces can be used to form these ordered molecular aggregates;[3,4] and chemical reactions between particles can also be used to form some ordered aggregates.[5,6] Research into the ordered self-assembly of functional molecules is very active, with potential applications in photonic and electronic devices.[7]

π-Conjugated molecules are endowed with characteristic electronic and optical properties because of their fairly delocalized (moving) electrons. Well-defined π-conjugated molecules are often investigated to obtain insight into the relationship between structure and electronic properties.[8] The great advantages of small π-conjugated molecular systems, namely, ready availability, ease of synthesis, and high purity, render them attractive components for device applications in, for example, light emitting diodes, light modulators, and field

Received: November 4, 2013
Published: March 25, 2014

   dx.doi.org/10.1021/ar400264e | Acc. Chem. Res. 2014, 47, 1186–1198

effect transistors.[9,10] To realize expected functions, both the chemical composition of the π-conjugated molecules and the degree of organization or alignment of their molecular chains must be controlled. Controlling the different hierarchies of the aggregates, from molecules to devices, is the most critical issue.[11,12] The planar geometries in π-conjugated molecules allow the formation of stacked assemblies; interchain electronic coupling will determine the performance of π-conjugated systems within electronic devices.[13]

Compounds that undergo intramolecular charge transfer (ICT) are typically π-conjugated systems that feature an electron donor (D) and an electron acceptor (A) connected through a π-conjugated bridge. In the solid state, the properties of ICT compounds are determined not only by the intrinsic features of their component moieties but also by their molecular packing.[14] Control over the relative orientation of the component parts and subtle modulation of intermolecular overlap are very important aspects for ensuring desired functions. ICT interactions are used widely to construct low-dimensional organic and organic/inorganic hybrid nanomaterials[15−18] and related supramolecular systems.[19] The D/A dipole−dipole interactions between ICT molecules have recently been used as a facile but valid force to induce the growth of organic nanostructures.[20,21] The assembly of strongly polarized red-emitting dyes into morphologically controllable nanostructures for use in light-emitting nanodevices and biological nanosensors has been successful when overcoming the aggregation-caused emission quenching (ACQ) effects of these materials.[22] Designing additional ICT compounds with structural and functional diversity and tailorability is a promising means of fabricating well-formed supramolecular architectures with desirable sizes, shapes, and functions.

In this Account, we summarize our attempts at designing organic ICT molecules that can be used to develop novel self-assembled materials, driven by their unique properties. We describe techniques for precisely controlling the sizes, shapes, and morphologies of these ICT compounds as well as understanding their self-assembly processes. Finally, we discuss the optical properties of these systems and how supramolecular sensor systems can be developed based on the tunable ICT processes of ICT chromophores.

2. THE NATURE OF ICT

Charge transfer (CT) is an important feature in several chemical and biological processes.[23] A CT complex or electron D/A complex is formed through the association of two or more molecules (intermolecular) or of different parts of one large molecule (intramolecular), with a portion of the electronic charge being transferred between the molecular entities.[24] Upon CT, a pair of ions is generated, with the D moiety becoming cationic and the A moiety becoming anionic. The resulting electrostatic attraction provides a force that stabilizes the molecular assembly. Many such complexes can undergo an electronic transition into an excited electronic state. The excitation energy of this transition often occurs in the visible region of the electronic spectrum, forming a feature described as a CT band, leading to a characteristically intense color for such molecules. For ICT in the excited state, several models have been discussed in the literature based on the molecular structure of the final state reached upon photoinduced ICT, including planar intramolecular charge transfer (PICT) or twisted intramolecular charge transfer (TICT).[25] For example, ICT has been proposed as being responsible for the strongly Stokes-shifted additional fluorescence band of fluorescent molecules featuring two fluorescence bands (dual fluorescent molecules). Resonance Raman spectroscopy[26] is also a powerful technique for analysis of CT bands in these ICT systems.

The ability to control the degree of CT in a π-conjugated push−pull system is a key factor for ensuring practical applications, such as the design of nonlinear optical (NLO) materials.[27] For a donor−bridge−acceptor (D−B−A) system, ICT is influenced by the nature of both the bridge and the substituents. The degree of ICT for a push−pull system can be estimated from the electronegativities and polarizabilities of the push and pull systems. In particular, when the D moiety is highly electropositive, the polarizability of the A moiety becomes a critical factor affecting the degree of ICT.[28] The rate of CT through insulating molecular spacers depends strongly on the nature of the chemical bonding of the spacer.[29] These principles provide us with facile strategies for the design of novel ICT compounds and for the assembly of ICT compounds with expected functions, as well as development of smart sensor systems based on tuning of the ICT processes.

3. DESIGN AND SYNTHESIS OF ICT COMPOUNDS

The design and synthesis strategy of the ICT compounds is an important topic for controlled self-assembly of novel functional molecular systems. This Account discusses the assembly characteristics of a series of ICT compounds that is held together with π−π interactions and other weak intermolecular interactions such as hydrogen bonding, CH−π, electrostatic, van der Waals, and dipole−dipole interactions. These aromatic molecules are composed of normal aromatic chromophores (such as perylene bisimide, benzothiadiazole, or oligo(*p*-phenylene vinylene)) substituted by functional groups. The design principle explored was how to use the functional groups for these compounds to tune the intramolecular charge transfer characteristics and supply supramolecular interactions for conformations that are predisposed to form 0- or 1-D nanostructures. Throughout the text, we will denote these ICT compounds by naming the core chromophores and following them by an Arabic numeral.

The introduction of heterocycles or heteroatoms to a π-conjugated system is a facile approach toward the construction of ICT compounds, with the lone pairs of electrons of the heteroatoms being used as electron donors. Substitution of OH groups on the bay region of perylene bisimide (PBI) renders a chromophore with ICT properties.[30] The J-aggregation properties of these dihydroxyperylene bisimides suggest the possibility of assembling nanostructures having specific dimensions and sizes. Whereas PBI-1 and PBI-2 form spherical particles having a uniform diameter of approximately 200 nm, the benzylimidazole-substituted compound PBI-3 provides hierarchical structures with right- and left-handed double-helical fibers (Figure 1). Introducing a nitrogen atom into the bay region of PBI has provided the compounds PBI-4 and PBI-5;[31] these N-heterocycle-annulated PBIs exhibit distinct optical and electronic properties because of significant electronic coupling between their heteroatom/heterocycles and their PBI cores. Phototriggered intramolecular cyclization of a 2-anthracene-substituted PBI enlarges the aromatic π-system of the PBI along its equatorial axis to provide novel ICT compounds,[32] in which strong ICT quenches the fluorescence of the linear compounds PBI-6. In the zigzag constitutional compounds PBI-7, twisting of the aromatic cores, driven by steric congestion between the

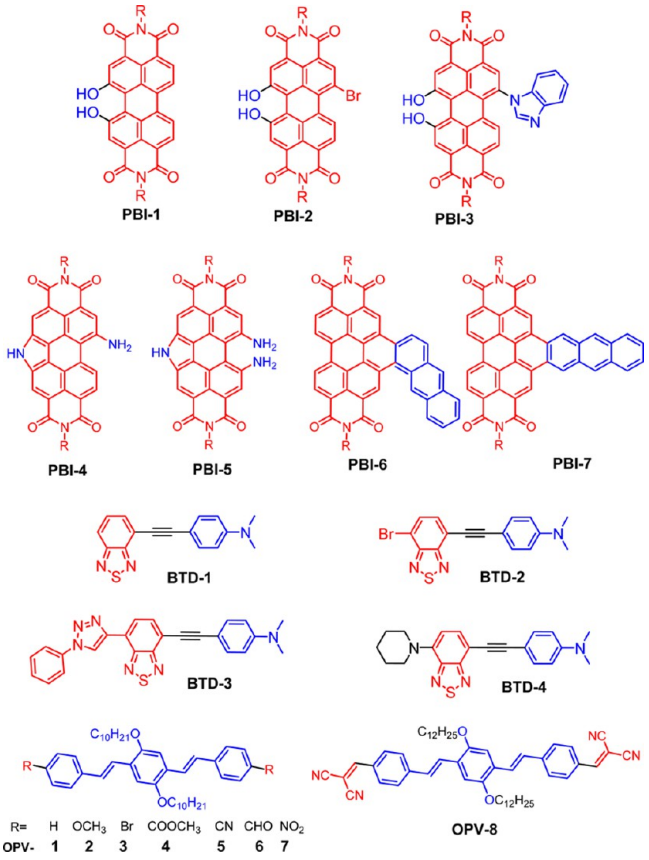

Figure 1. Molecular structures of several ICT compounds.

9-H atom of the anthracene unit and the neighboring hydrogen atoms on the perylene core, greatly decreases electronic communication between the anthracene and perylene units.

The nature of the substituent groups greatly influences the structural and photophysical properties of D/A molecules. For example, installation of a triazole moiety into the benzothiadiazole cores of *N*,*N*-dimethylaniline- and benzothiadiazole-based D/A molecules (BTD-1, BTD-2, BTD-3, BTD-4) can improve the optical properties and crystal packing of these benzothiadiazole derivatives.[33] Tuning of the emission color of bis-dipolar trimeric oligo(*p*-phenylene vinylene) (OPV) materials has been achieved through the appending of push−pull electron groups at the two ends (OPV-1−7).[34] Two cyano groups attached to both sides of the OPV gave OPV−8, with ICT processes occurring between the cyano groups and the OPV core.[35]

4. ASSEMBLY OF ICT COMPOUNDS INTO VARIOUS STRUCTURES

ICT compounds can be self-assembled into rather distinct solid superstructures driven by supramolecular interactions such as asymmetric and symmetric dipole−dipole interactions, axial coordination. The rapid [2 + 2] cycloadditions between tetracyanoethylene (TCNE)/7,7,8,8-tetracyanoquinodimethane (TCNQ) and alkynes substituted with electron-donating groups (EDGs) and electron-withdrawing groups (EWGs) have provided a series of ICT compounds, tetracyanobutadienes (TCBDs) (Figure 2). The OPV_3-bridged ICT compound TCBD-1 can undergo a morphological transition in its self-assembling process, from zero-dimensional (0D) hollow nanospheres to one-dimensional (1D) nanotubes.[22] The model ICT compound TCBD-2, which features the same D/A pairs as TCBD-1, can undergo a similar morphological transition from 0D to 1D nanostructures. Compound TCBD-3 undergoes a similar morphological transition and reconstruction process from 0D hollow nanospheres to 1D tubular microstructures.[36] The morphological transitions and reconstruction processes of these ICT compounds have been proposed as "curvature strain releasing" processes driven by D/A dipole−dipole interactions.[37] By controlling the axial coordination of zinc porphyrin with 4,4′-bipyridine, an amphiphilic porphyrin derivative DOCP-Zn has been utilized to construct tunable nanostructures from 0D to 1D.[38] The patterns conversion between 0D nanospheres and 1D nanorods or nanoslices can be reversibly realized by the construction or destroy of the axial coordination interaction.

The molecular structures such as the nature of the linkage between the D and A units influence the self-assemblied structures and photophysical properties of ICT compounds. The furan-substituted compounds PBI-8 and PBI-9 can be assembled into highly stable 0D nanospheres and 1D microrods, respectively (Figure 3). PBI-8 might initially precipitate at the interface between the two solvents and assemble into a curved surface with $\pi-\pi$ stacking aggregation between the D moiety (furan unit) and the A moiety (perylene plane); accordingly, nanospheres could be formed. After photocyclization at the bay region, the furan group extends the conjugation of the perylene core along the short molecular axis. With the enlargement of the aromatic core system, the ability of these aromatic molecules to undergo $\pi-\pi$ stacking was enhanced, resulting in uniform microrod structures.[39] The D/A molecules BTD-5 and BTD-6 contained carbazole moieties as their D moieties and a NO_2-substituted benzothiadiazole as their A moiety.[40] X-ray crystal data elucidated multiple intermolecular interactions in these systems. These interactions were the main driving forces directing the self-organization of the microstructures, with the different linkages exhibiting distinctly different self-assembly behavior. BTD-5 with benzene linkage preferred to form cubelike microstructures at room temperature (Figure 4a), while BTD-6 linked by benzenethynyl group formed rigid nanowires (Figure 4d). A series of D/A molecules with *N*,*N*-dimethylaniline or carbazole as the common electron D moiety and 3-phenyl-5-isoxazolone as the electron A moiety (ISO-1, ISO-2, ISO-3) has been synthesized to further study the affect of the D units and linker groups on the self-assembly and photophysical properties of ICT compounds.[41] Using phase transfer methodologies and solvent-vapor techniques, these compounds self-assembled into various superstructures, including ribbonlike architectures, hollow nanospheres, multilayer plates, and rhombic microplates (Figure 4g−o).

The operating parameters, such as the temperature, concentration, and growth time, greatly influence the morphologies of the molecular aggregates in the different self-assembled systems, due to the different types of hydrogen bonds and $\pi-\pi$ stacking interactions in the different chemical environments. The morphologies of the final architectures are also affected by the shape of the precursor crystal seeds.[42] The ICT molecules BTD-7 and BTD-8, which each feature a carbazole unit as the D moiety and a benzothiadiazole unit is the A moiety, have been designed to tune the molecular aggregate structures (Figure 5).[43] The controllable aggregate structures of these ICT compounds include highly uniform tubule-, rod-, and cubelike architectures, obtainable in large

dx.doi.org/10.1021/ar400264e | *Acc. Chem. Res.* 2014, 47, 1186−1198

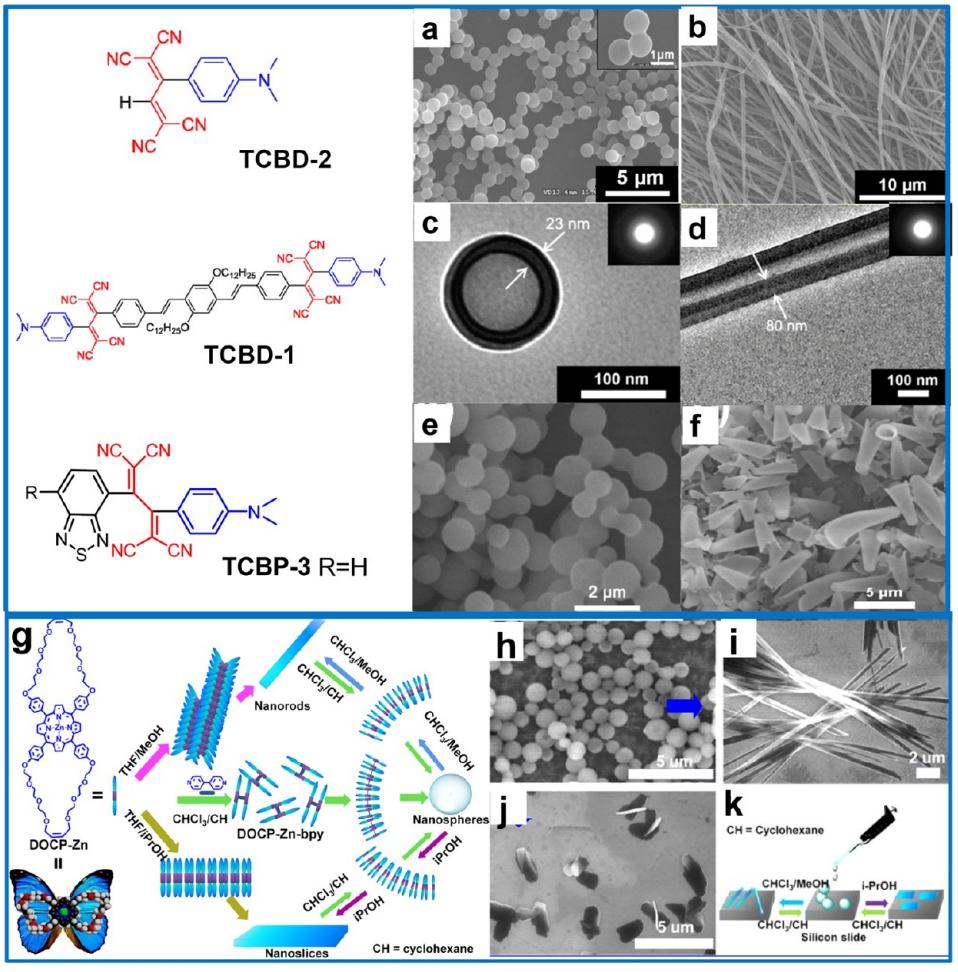

Figure 2. Morphological transitions of ICT compounds, from 0D to 1D nanostructures. SEM images of TCBD-2 nanospheres (a) and 1D nanowires (b). TEM images of TCBD-1 hollow nanospheres (c) and 1D nanotubes (d). Reprinted with permission from ref 22. Copyright 2008 American Chemical Society. SEM images of compound TCBD-3 0D hollow nanospheres (e) and 1D tubular microstructures (f). Schematic outline of the aggregate structure conversion procedure (g). SEM images of the nanostructures of DOCP-Zn-bpy complex in $CHCl_3$/cyclohexane (v/v 1:1) (h) and pattern conversion from nanospheres to nanorods in $CHCl_3$/MeOH (v/v 1:1) (i) or nanoslices in *i*-PrOH (j), and experimental procedure (k). Adapted from refs 22, 36, and 38.

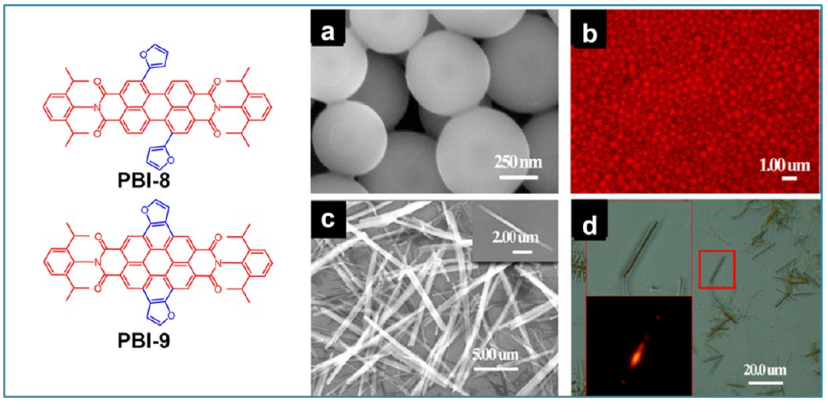

Figure 3. (a) SEM and (b) LSCM images of PBI-8 aggregates and (c) SEM and (d) PL microscopy images of PBI-9 aggregates prepared at room temperature in CH_2Cl_2/MeOH (1:1, v/v). Adapted from ref 39.

quantities and with high morphological and chemical purity. For BTD-7, the crystallization occurred at the interface between the THF and hexane layers, which functioned as a soft template. The rate of crystallization at the interface between the two phases was higher than that for the diffusion of BTD-7 from the THF phase into the hexane phase because of the poor solubility of BTD-7 in hexane. Therefore, BTD-7 tends to stack along the *c*-axis, due to strong $\pi-\pi$ interactions and hydrogen bonds. The tubular structure readily formed along the growth direction of the template wall. The growth rates along the wall exceeded the growth rate in the middle of the template; at the same time, redissolving occurred initially at

dx.doi.org/10.1021/ar400264e | *Acc. Chem. Res.* 2014, 47, 1186−1198

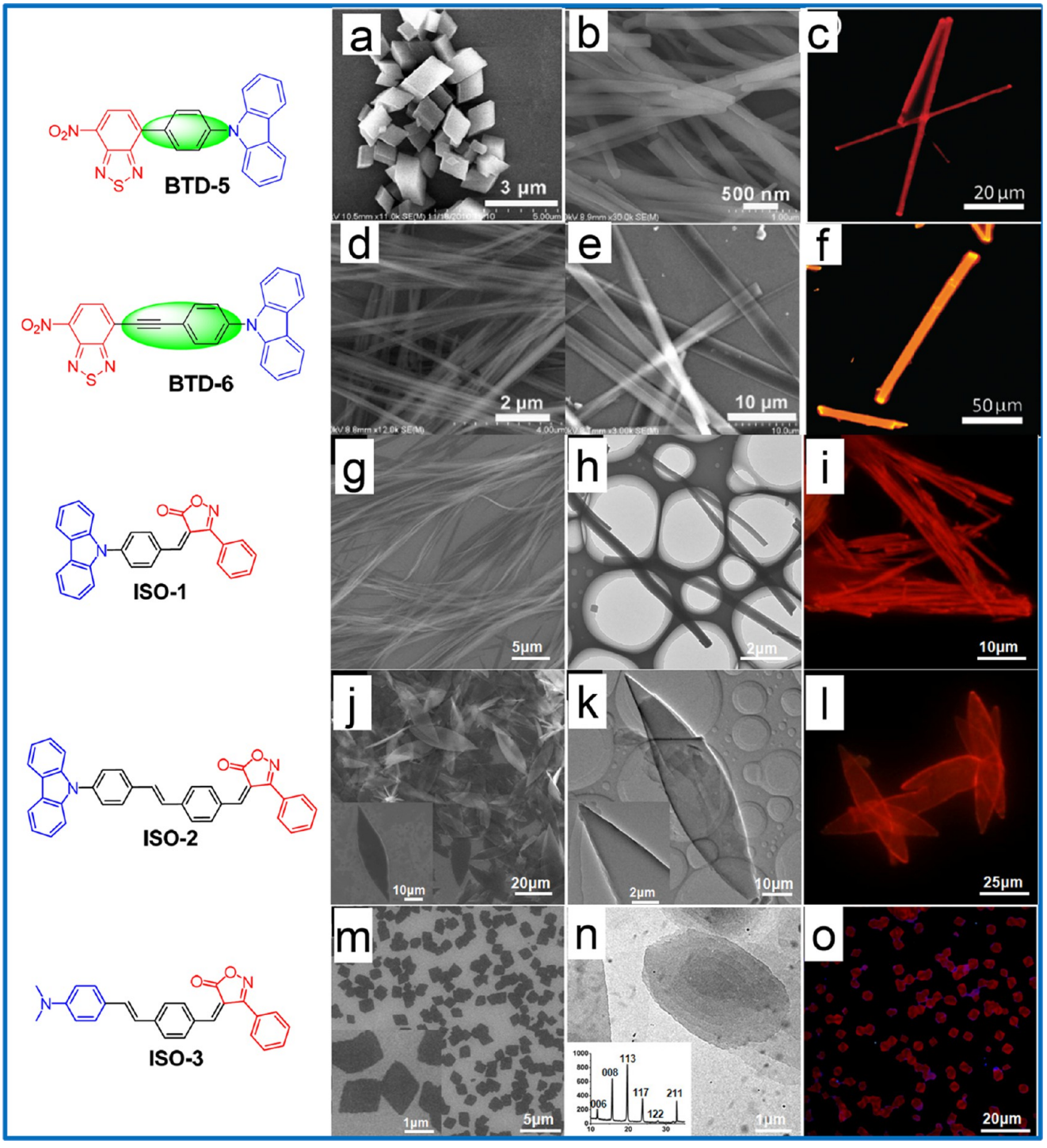

Figure 4. (a) SEM images of cubiclike microcrystals and (b) nanowires of BTD-5; (d) nanowires and (e) microrods of BTD-6, SEM and TEM images of (g, h) ISO-1, (j, k) ISO-2, (m, n) ISO-3. Confocal fluorescence microscopy images of (c) BTD-5, (f) BTD-6, (i) ISO-1, (l) ISO-2, and (o) 7 excited with a UV band (330−380 nm) light source. Adapted from refs 40 and 41.

the center of the high-energy facet, due to its surface energy being the highest among all of the facets of the 1D aggregate, and then continued toward the inside along the *c*-axis. As a result, a perfectly crystalline tubule-like structure resulted. In contrast, the growth rates and growth directions of the molecular aggregates were identical when using EtOH/THF as the soft template, due to weakened hydrogen bonding interactions; accordingly, 1D rod-like structures were obtained.

The temperature also greatly influenced the formation of the nanostructures. BTD-5 formed cubelike microcrystals from a saturated THF solution at room temperature (Figure 4a), whereas 1D nanowires were assembled at elevated temperature (Figure 4b). BTD-6 formed rigid nanowires after injection of its saturated THF solution into vigorously stirred hexane (Figure 4d). In contrast, 1D microrods were observed after cooling a saturated THF solution of BTD-6 naturally from under reflux

dx.doi.org/10.1021/ar400264e | *Acc. Chem. Res.* 2014, 47, 1186−1198

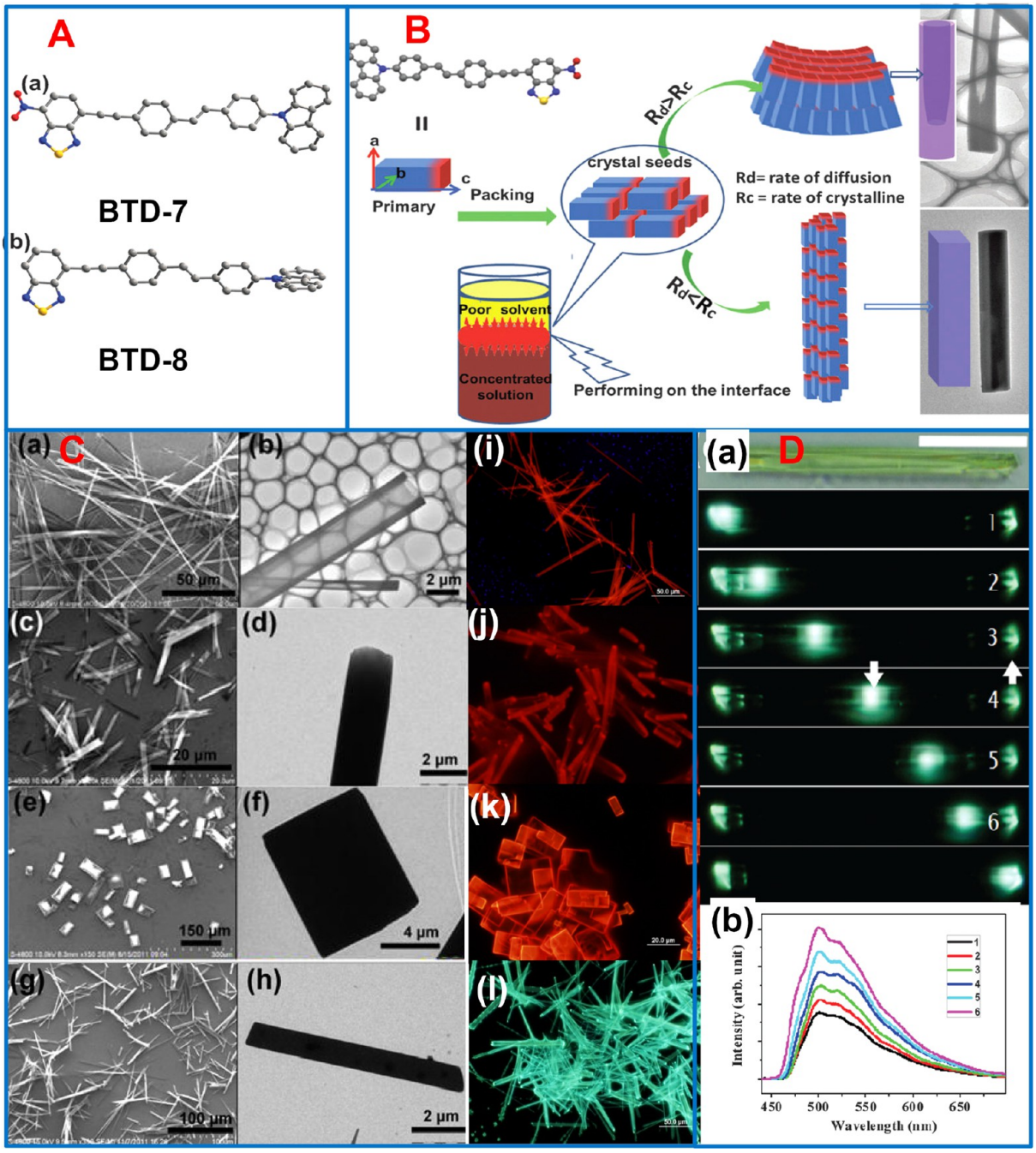

Figure 5. (A) Crystal structures of (a) BTD-7 and (b) BTD-8. (B) Schematic representation of the self-assembly processes of BTD-7. (C) Large-area SEM, TEM, and confocal fluorescence microscopy images of (a–f, i–k) BTD-7 (a, b, i) microtubes, (c, d, j) microrods, (e, f, k) microcrystals; and (g, h, l) BTD-8 microrods. (D) (a) Microarea PL images obtained after exciting a microrod at different positions; down arrow, excited site; up arrow, emitted tip; scale bar, 20 mm. (b) Corresponding PL spectra in (c). Adapted from ref 43.

(at 70 °C) to 25 °C in an oil bath and keeping the system undisturbed for more than 6 h (Figure 4e).

Controlling the concentration and growth temperature allows the D/A molecule tripyrenylborane TPB to readily form solid supermolecular structures, including 1D nanowires, nanofibers, and nanorods (Figure 6). Triarylboranes react with small nucleophilic fluoride anions because of their intrinsic Lewis acidity, resulting in modulation of the CT interactions between the pyrene unit and the B atom. Upon the addition of fluoride, the absorption bands of TPB near 275 and 345 nm weakened and a new absorption band appeared at 440 nm; in addition, the emission bands of TPB near 385, 405, and 427 nm weakened and a new red-shifted emission band appeared at 450 nm. The fluorescence quenching properties of TPB solid materials upon the addition of fluoride ions indicate that TPB materials have potential applications in the detection and separation of fluoride anions.[44]

The molecular aggregation of ICT compounds can also be controlled in supramolecular systems (e.g., molecular shuttles).[45] The ICT compound TCBD can form regular nanostructures by virtue of intermolecular dipole–dipole interactions.[22] After attachment of TCBD to the threadlike component of a molecular shuttle, the aggregation behavior of the TCBD unit could be modulated by the shuttling movement

dx.doi.org/10.1021/ar400264e | Acc. Chem. Res. 2014, 47, 1186–1198

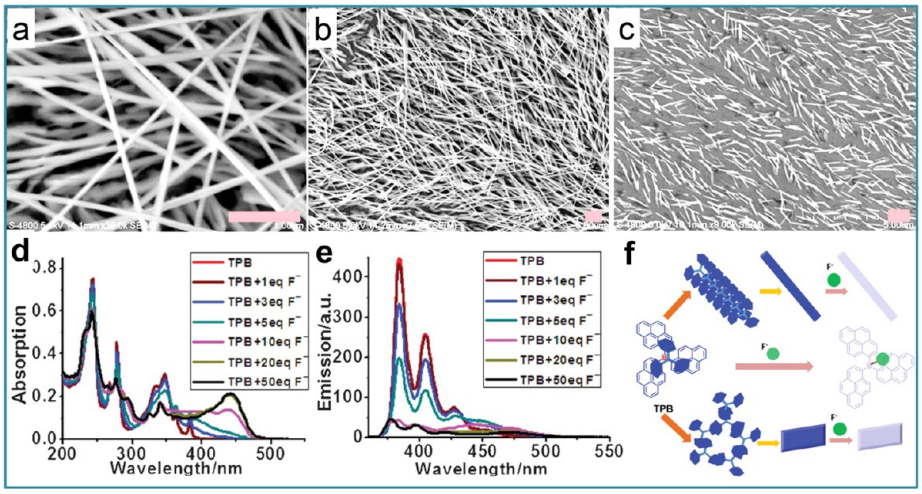

Figure 6. SEM images of self-assembled TPB structures on silicon slices, prepared in THF/MeOH (v/v, 1:1) at temperatures of (a) 25 °C (nanowires), (b) 40 °C (nanofibers), and (c) 40 °C (nanorods). Concentration of TPB: (a, b) 5×10^{-4} M; (c) 2×10^{-4} M. (d) UV–vis and (e) fluorescence spectra of TPB (5×10^{-5} M in CH_2Cl_2) upon titration with *n*-Bu_4NF from 0 to 50 equiv. (f) Schematic representation of the aggregation of TPB and of the solid blue-fluorescence quenching in the presence of fluoride anions. Adapted from ref 44.

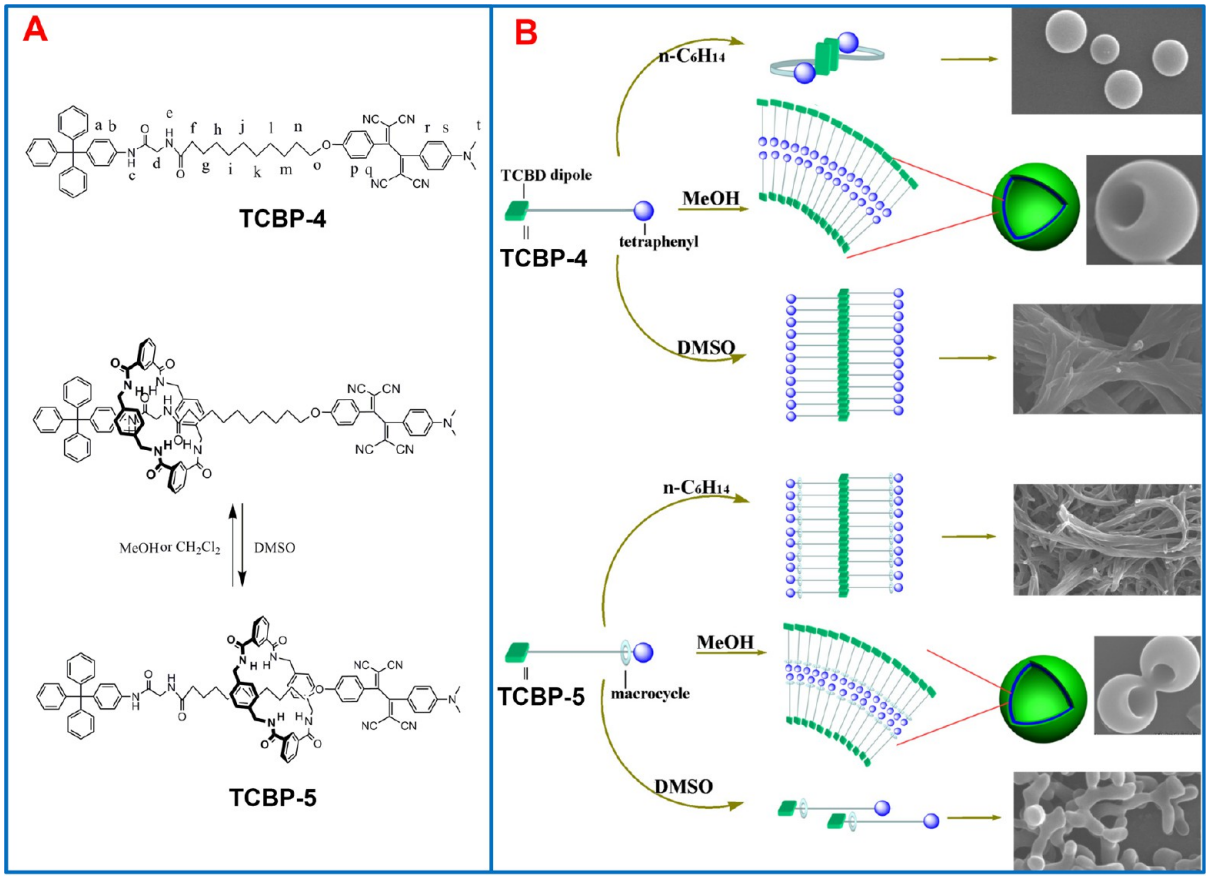

Figure 7. (A) Chemical structure of a molecular shuttle presenting an attached ICT chromophore unit. (B) Self-assembly of TCBD-4 and TCBD-5 under various conditions. Adapted from ref 45.

of the macrocyclic component along the threadlike component (Figure 7). For the threadlike unit itself (TCBD-4), the aggregation behavior of the TCBD unit is controlled solely by the choice of solvent. In the [2]rotaxane TCBD-5, the macrocyclic component can be positioned close to or far from the TCBD unit upon changing the solvent polarity; thus, the aggregation behavior of the TCBD unit is also influenced significantly by the movement of the macrocyclic component. The macrocyclic component resided at the peptide station in a mixed solvent of $CHCl_3$/*n*-C_6H_{14} (1:1, v/v); interlaced nanofibers were formed because of the intermolecular dipole–dipole interactions of the TCBD units. In $CHCl_3$/MeOH (1:1, v/v), although the macrocyclic component was located at the peptide station, perforated capsules were formed

dx.doi.org/10.1021/ar400264e | *Acc. Chem. Res.* 2014, 47, 1186–1198

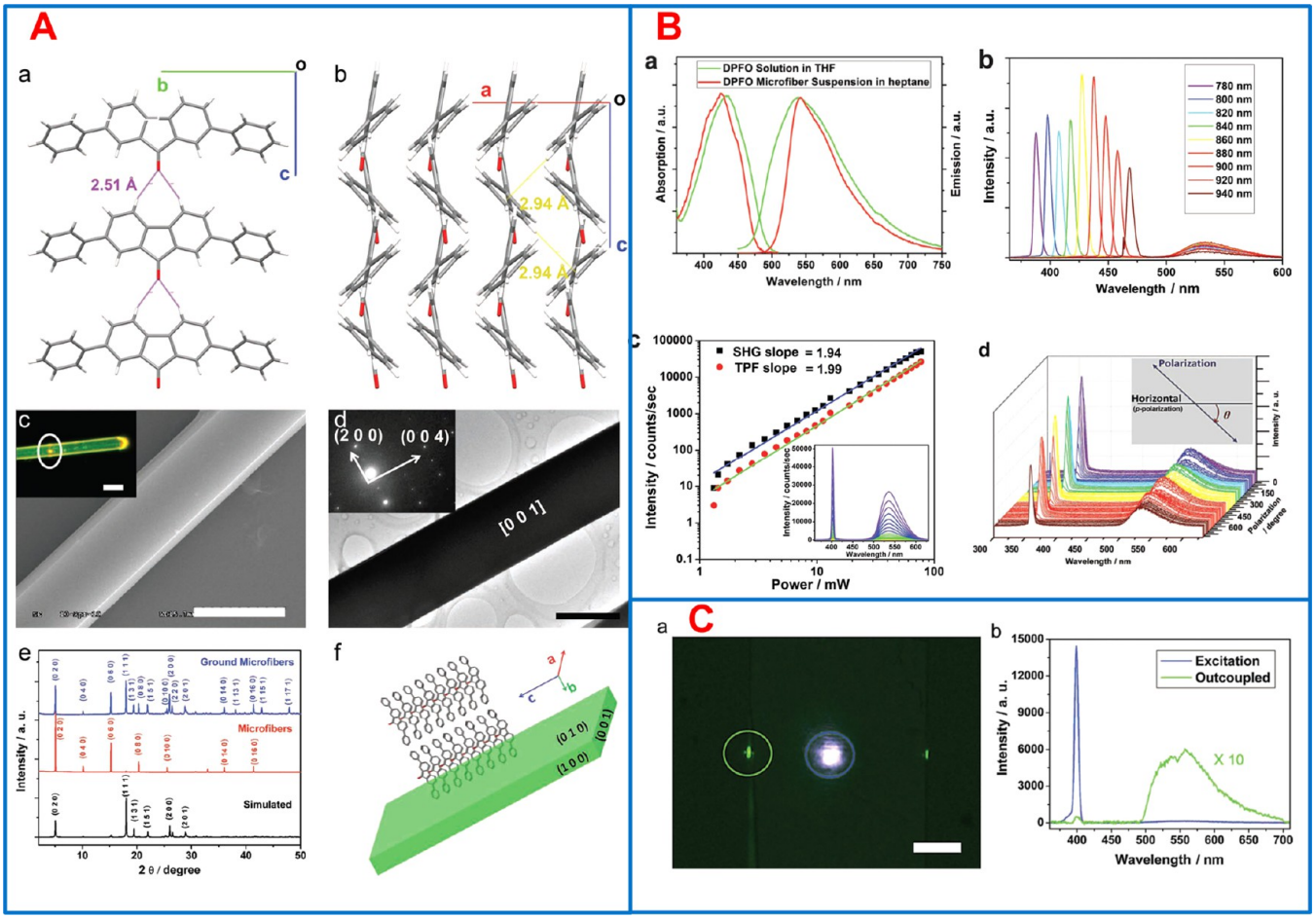

Figure 8. (A) Morphology and molecular packing of DPFO microfibers. (B) Linear and nonlinear optical responses of DPFO. (a) UV–vis absorption and PL spectra of DPFO in solution and in the aggregation state. (b) Spectra collected from a fixed spot of a microfiber when pumped at different wavelengths, normalized by the power of the input laser. (c) Logarithmic plots of the power dependence of SHG and TPF. (C) Waveguiding behavior of SHG and TPF. (a) Microscopy image of a DPFO microfiber excited in the middle spot; excitation, 800 nm; substrate, MgF_2; scale bar, 5 μm. (b) Corresponding spectra of the excitation spot (blue circle) and outcoupled spot (green circle). Adapted from ref 50.

as a result of the amphiphilic properties of the molecular structure. In DMSO, wormlike nanoparticles were obtained because the macrocycle obstructed the intermolecular dipole–dipole interactions of the TCBD units. Therefore, the aggregation behavior of ICT compounds can be controlled by the shuttling movement of macrocyclic components in molecular shuttles.[45]

These parameters influenced the thermodynamic equilibrium for self-assembly, which induced assembly structural difference. Based on concepts of crystal growth, the nucleation sites, the nucleation rate, and the growth rate can be influenced by assembly solvents, growth temperature, and concentration of the precursor.[46] From the above discussion we can say that the molecular structures control the morphology and the precursor concentration controls the nucleation density, while the temperature controls the aspect ratio and morphology. For solvents with strong interactions with the precursors would influence the molecular packing styles, while for the solvents with little interactions with the precursors would mainly control the growth rate of the aggregate and then control the aspect ratio. Nevertheless, only one parameter was considered. We believe that the morphological and structural characteristics of the assembled aggregates can be controlled by simply tuning the above-mentioned growth parameters.

5. ASSEMBLY OF ICT COMPOUNDS WITH TUNABLE OPTICAL PROPERTIES

The properties of ordered molecular assemblies can vary from those of their individual constituent molecules.[2−5] The photophysical properties of π-conjugated compounds in the solid state depend largely upon their mode of molecular packing, which can be tuned by various noncovalent forces. For example, the relative positions of adjacent molecules and the directions of their dipole moments can strongly influence luminescence, exciton migration, and carrier mobility. Well-ordered porphyrin films have exhibited a saturation absorption having a nonlinear absorption coefficient (β) of -4.3×10^{-6} m W^{-1} and a nonlinear refraction coefficient (η_2) of 2.8×10^{-13} m^2 W^{-1}; this latter value is 3 orders of magnitude greater than that measured in solution.[47]

ICT compounds possessing high hyperpolarizabilities are employed widely as second- and/or third-order NLO chromophores.[48] The main requirement for the development of a material for second-harmonic generation (SHG) from these ICT compounds is that the NLO chromophores should be arranged noncentrosymmetrically.[49] Having synthesized the V-shaped fluorenone-based ICT compound 2,7-diphenyl-9*H*-fluoren-9-one (DPFO),[50] we obtained microcrystals with widths ranging from several to tens of micrometers and lengths

dx.doi.org/10.1021/ar400264e | *Acc. Chem. Res.* 2014, 47, 1186–1198

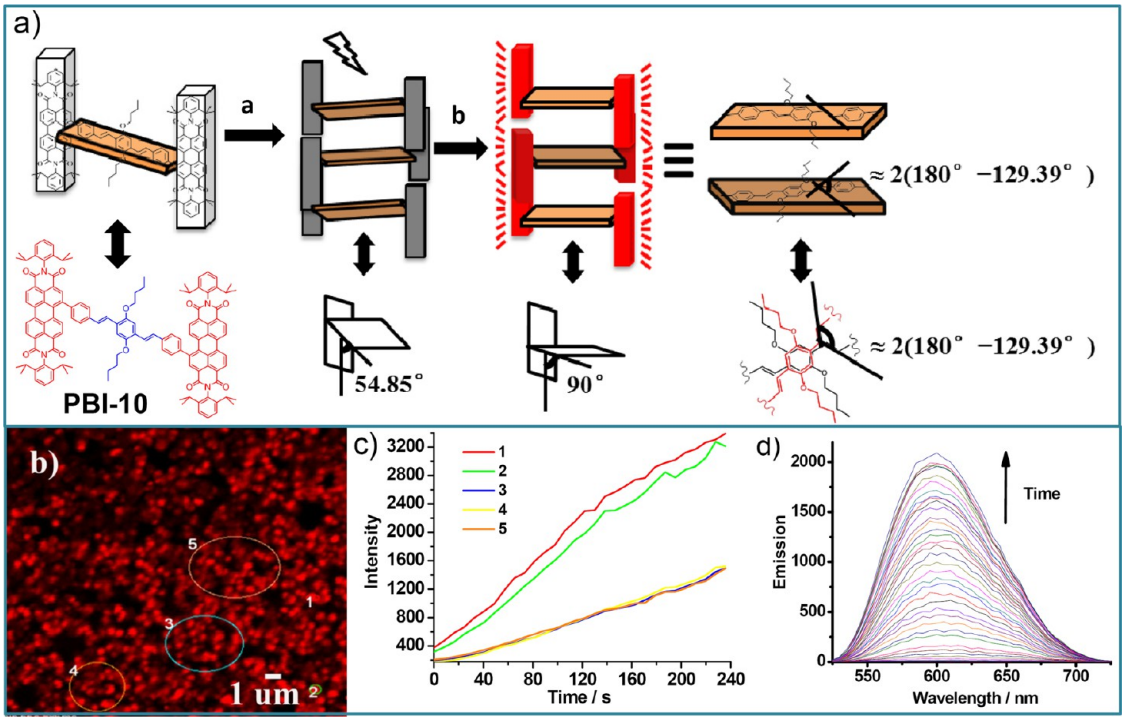

Figure 9. (a) Proposed mechanism for the fluorescence emission enhancement of PBI-10 after self-assembly induced by the special wavelength of the laser. (b, c) Time-dependent intensity plot of the fluorescence emission and (d) time-dependent emission spectra of self-assembled spherical nanoparticles of PBI-10. Adapted from ref 51.

of up to several millimeters (Figure 8A-c). The single crystals of the DPFO fibers were indexed with the bulk-crystal lattice constants, suggesting that the microfibers grew along the [001] direction (Figure 8A-d). Powder XRD of the microfibers indicated that the thin axis of the microfiber perpendicular to the substrate was the *b*-axis (Figure 8A-e). Noncovalent interactions among DPFO molecules along the different crystallographic axes led to these thin and long microfibers (Figure 8A-f). The molecular dipoles contributed to the macroscopic permanent dipole moment of the microfiber: the long axis of the microfibers was the crystallographic *c*-axis and the permanent dipole of the molecules was also directed along this direction.

The molecular dipolar structure of DPFO and the *Ccm*2 1 space group results in strong second-order NLO properties. At half the wavelength of the incident beam, a sharp SHG band was observed, while a much broader band was observed at higher wavelength (Figure 8B-b).[50] The broad band is similar to the fluorescence spectrum; it is attributed to two-photon fluorescence (TPF). Although the wavelength of the SHG band depended on the frequency of the incident laser, the TPF was always fixed at 530 nm and exhibited a variation in only the intensity of the peak (Figure 8B-b). Power-dependence measurements (Figure 8B-c) revealed that the intensities of both the SHG and TPF signals scaled quadratically with the power of the input laser, confirming that both NLO processes originated from two-photon excitation. The intensities of the SHG and TPF signals could be tuned conveniently through changes in the polarization and incidence angle of the light (Figure 8B-d). The unusual extremely high polarization ratio for an organic material makes DPFO ideal for use in logic devices. Furthermore, its SHG and TPF signals can readily be separated macroscopically by taking advantage of their different waveguiding behaviors. The combination of polarization and waveguiding effects provided us with the opportunity to up-convert to different frequencies at different locations within the same sample. For example, a bright blue spot appeared at the excitation location of the fiber when pumped at 800 nm, while the green TPF propagated to the edges of the microfiber (Figure 8C-a).[50] Spectra recorded from the excitation spot of the microfiber and the guided spot at the edge of the microfiber (Figure 8C-b) revealed that the SHG signal was obtained exclusively at the excitation spot, whereas the TPF signal was observed only at the guided spot. The highly directional properties of SHG led to its nonpropagation. The TPF signal, however, readily propagated to the edges of the microfiber, indicating that this microfiber acted as a waveguide for this emitted light. We could tune independently the intensity of either the SHG or TPF signal. Thus, the orientation of dipoles is an important and essential design parameter for future organic NLO materials.

Most D/A-substituted compounds suffer from ACQ in the solid phase, greatly limiting their applications. We have observed aggregation-induced emission (AIE) effects for several of our ICT compounds, including the carbazole- and benzothiadiazole-based BTD-7 and BTD-8 (Figure 5); the *N*,*N*-dimethylaniline- and benzothiadiazole-based BTD-1 (2, 3, 4), BTD-5, and BTD-6 (Figure 4); TCBD-1; and the 3-phenyl-5-isoxazolone-based ISO-1, ISO-2, and ISO-3 (Figure 4). These prepared nanostructures exhibit green, yellow, and especially red emissions. In addition, the distance-dependent photoluminescence image of a single microrod of BTD-8 measured using a near-field scanning optical microscope indicated that these microrods possess outstanding optical waveguide properties, with a waveguide efficiency (a) of 0.018 dB μm^{-1} and no obvious red-shift (Figure 5D).[43] The furan-substituted perylene bisimide PBI-9 also possesses good optical waveguide proper-

dx.doi.org/10.1021/ar400264e | *Acc. Chem. Res.* 2014, 47, 1186−1198

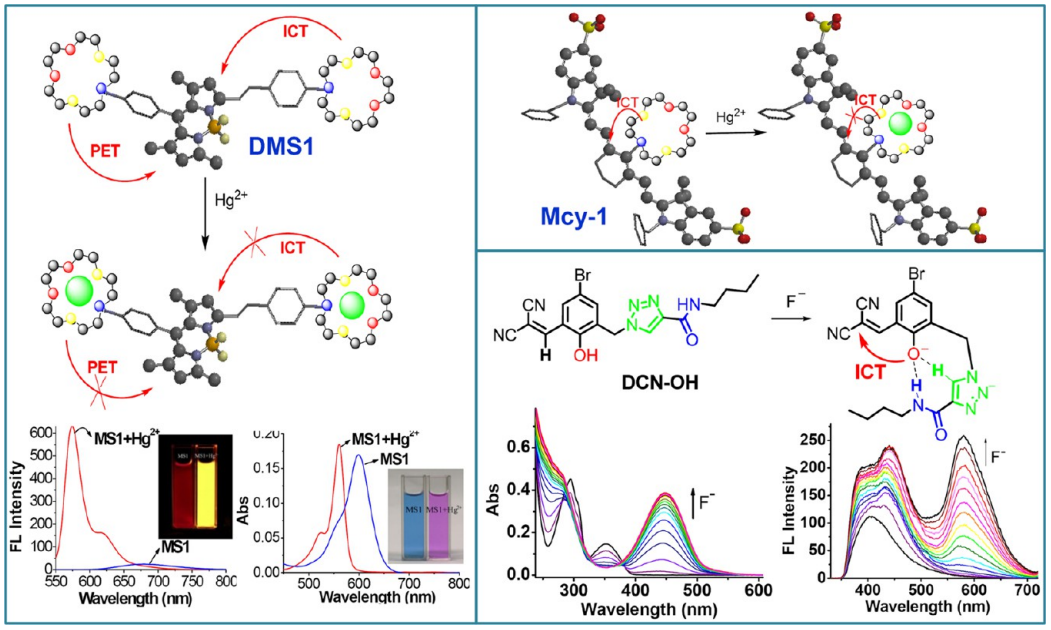

Figure 10. Tuning ICT processes through complexation with cations or anions. Adapted with permission from refs 52 (Copyright 2007 American Chemical Society), 53 (Copyright 2008 American Chemical Society), and 54.

ties (inset of Figure 3d). These materials have potentially highly interesting applications in optical devices.

The self-assembly of a new *p*-phenylenevinylene–linked perylene diimide, PBI-10, in CH_2Cl_2/hexane leads to 0D nanospheres having a diameter of approximately 800 nm (Figure 9b).[51] From studies of the fluorescence enhancement behavior of PBI-10 induced by laser irradiation, we proposed a conformation-dependent mechanism.[51] First, because of intermolecular steric clashes of the 2,6-diisopropylphenyl groups and intermolecular van der Waals interactions among the oxyalkyl chains, PBI-10 stacks with an angle of approximately 101° between two adjacent intermolecular double bonds with the face-to-face $\pi-\pi$-stacked middle benzene ring as a center; this style is repeated every two adjacent molecules (Figure 9). Second, under irradiation from a laser at 515 nm, the molecules obtain sufficient energy to overcome the rotational energy barrier and rotate on their axes to and fro at the balance position; that is, the molecules change from one conformation to another. Because of the steric bulk of adjacent molecules in the self-assembled solid state, the molecule rotates to a position in which the *p*-phenylenevinylene unit is almost perpendicular to both sides of the perylene units and is stuck fast and frozen; this alignment decreases interactions between the D (*p*-phenylenevinylene) and A (perylene) moieties, thereby leading to the appearance of the emission of the J-stacked perylene diimide itself. This mechanism differs from the fluorescence bleaching of normal solid-state-fluorescent materials; accordingly, such materials have interesting potential applications in optical devices.

Binding of some chemical species to the D or A moieties of ICT compounds can affect the efficiency of ICT processes, resulting in changes in dipole moments.[25] Indeed, Stokes shifts of the fluorophores and changes in quantum yields and fluorescence lifetimes are often observed. Thus, it is possible to design molecular sensors that function based on changes in the efficiency of an ICT process. For a BODIPY (4,4-difluoro-4-bora-3a,4a-diaza-*s*-indacene) chromophore functionalized with two dithiadioxaaza macrocycles, photoinduced electron transfer (PET) and ICT have both been invoked to rationalize its fluorescence response toward Hg^{2+} ions (Figure 10).[52] The optical absorption spectra of compound DMS1 exhibits an absorption maximum at 606 nm, a red-shift, due to ICT, of approximately 100 nm relative to that of BODIPY itself. The addition of Hg^{2+} ions led to a hypsochromic shift of the absorption maximum to 564 nm, tuning the color of the solution from purple to red-pink. ICT from the nitrogen atom of the D moiety of the macrocycle to the BODIPY chromophore led to the red-shift of the emission of this compound relative to that of unfunctionalized BODIPY. Coordination of a Hg^{2+} ion to the dithiadioxaaza macrocycle decreases the electron donating ability of the nitrogen atom and disrupts the ICT process, leading to a hypsochromic shift of the emission band. In addition, PET quenching of the BODIPY excited state by the lone pair of electrons of the nitrogen atom was alleviated upon complexation of the Hg^{2+} ion, thereby inducing fluorescence enhancement. DMS1 can be used for the ratiometric detection of Hg^{2+} in terms of both fluorescence and color changes. By tuning the ICT process, we also constructed a new type of near-infrared (NIR) probe, Mcy-1, that functions, through a colorimetric assay, to detect Hg^{2+} ions specifically (Figure 10).[53] An efficient excited state ICT process from the nitrogen atom of the D unit on the dithia-dioxa-monoaza macrocycles to the tricarbocyanine group of the A unit leads to a blue-shift of 88 nm of the absorption of Mcy-1 relative to that of the parent dye. Upon the gradual addition of Hg^{2+} ions, the intensity of the absorption band of Mcy-1 at 695 nm decreased sharply, while the intensity of a new band at 817 nm increased prominently with a single isosbestic point at 740 nm. The coordination of the Hg^{2+} ion to the ligand decreased the electron donating ability of the nitrogen atom at the macrocycle; as a result, the ICT process could not occur and the blue-shift in the absorption spectra was suppressed. A blue solution of Mcy-1 becomes almost colorless upon titration with Hg^{2+} ions, thereby providing the possibility of detection of Hg^{2+} ions with the naked eye. Prevention of excited-state ICT

dx.doi.org/10.1021/ar400264e | *Acc. Chem. Res.* 2014, 47, 1186–1198

from the D unit to the A unit induced a strong decrease in fluorescence upon complexation with Hg^{2+} ions.

In addition to cation sensing, the sensing of anions can also be realized through tuning of ICT processes. For DCN-OH, which contains an electron-poor 2,2-dicyanovinyl group, deprotonation of the OH group resulted in a red-shift of the CT band, arising from the electron-rich phenoxide unit to electron-poor dinitrile moiety, in the UV−vis spectrum (Figure 10).[54] A dramatic change in color, from colorless to yellow, occurred upon the addition of tetrabutylammonium fluoride to a solution of DCN-OH; the intensity of the emission band at 408 nm increased gradually along with the simultaneous growth of a new strong emission band at 580 nm, which is ascribed to a TICT state resulting from internal rotation of the dicyanovinyl group with respect to the benzene ring being limited upon the formation of intramolecular hydrogen bonds between the phenoxide anion and the dicyanovinyl H_c atom or the triazole CH unit. Thus, a colorimetric fluorescence chemosensor was obtained.

6. CONCLUSIONS AND PERSPECTIVES

This Account covers progress in the synthesis, self-assembly, and properties of functional molecular systems with well-defined assembled structures based on CT interactions. The rational design of ICT molecules that are easy to assemble and display clear structure−property relationships can be employed to develop novel functional systems. We have reviewed new methods for synthesizing ICT compounds through the introduction of heterocycles or heteroatoms to π-conjugated systems or through extending the conjugation of diverse aromatic systems using other aromatic rings. The various D/A moieties and different linkages of ICT compounds greatly influence the morphologies and sizes of the organic aggregates, as well as their photochemical properties. For example, independent NLO responses can be separated and tuned spectroscopically and spatially in noncentrosymmetric microfiber structures; another application for ICT compounds is the development of molecular sensors that function based on tuning of the efficiencies of ICT processes. Despite great achievements in functional molecular systems based on CT interactions, especially for controllable aggregate nanostructures of ICT molecules with foreseeable applications in the fields of electronics, optics, and optoelectronics, many challenges remain. Further research will certainly increase our understanding of these fundamental processes and their applications. The search for highly efficient reactions for the construction of stable, stimulus-responsive molecular systems based on ICT remains one challenge; another is controlling the alignment of the functional chromophores symmetrically or noncentrosymmetrically. Theoretical methods for predicting the preferred geometries of assemblies and the use of such approaches as macromolecular scaffolding, field-assisted poled-polymer alignment, and modern crystal engineering should be investigated to generate the expected macroscopic arrangements. We believe that new or improved chemical and physical properties, induced through controlled self-assembly of ICT compounds, will continue to be exploited for applications in optics, electronics, and optoelectronics.

AUTHOR INFORMATION

Corresponding Authors

*E-mail: liuhb@iccas.ac.cn.

*E-mail: ylli@iccas.ac.cn. Fax: (+) 86-10-82616576. Tel: (+) 86-10-62587552.

Author Contributions

The manuscript was written through contributions of all authors. All authors have given approval to the final version of the manuscript.

Notes

The authors declare no competing financial interest.

Biographies

Dr. Yongjun Li received his Ph.D. degree in 2006 from the Institute of Chemistry of the Chinese Academy of Sciences (ICCAS). He is currently an Associate Professor in Professor Yuliang Li's group at ICCAS, designing and synthesizing functional organic molecules.

Dr. Taifeng Liu received his Ph.D. from ICCAS, under the direction of Professor Yuliang Li (2013). He is now a project staff in Li's group working on supramolecular self-assemblies of π-conjugated organic molecules.

Prof. Huibiao Liu received his Ph.D. degree in 2001 from Nanjing University. He is currently a Professor at ICCAS, studying inorganic/organic hybrid nanomaterials and nanoscale and nanostructural materials.

Dr. Mao-Zhong Tian received his Ph.D. from Dalian University of Technology (2008). Currently, he is a Senior Visiting Scholar in Prof. Li's group at ICCAS.

Prof. Yuliang Li is a Professor at ICCAS. His research interests lie in the field of design and synthesis of functional molecules, self-assembly methodologies of low dimension and large size molecular aggregations structures, chemistry of Carbon and rich carbon, with particular focus on the design and synthesis of photo-, electro-active organic−inorganic hybrid materials and nanoscale and nanostructural materials.

ACKNOWLEDGMENTS

Our contributions in this Account were realized with support from the National Nature Science Foundation of China (21031006, 91227113, 21322301), the NSFC-DFG joint fund (TRR 61), and the National Basic Research 973 Program of China.

REFERENCES

(1) Zhao, Y.; Fu, H.; Peng, A.; Ma, Y.; Liao, Q.; Yao, J. Construction and Optoelectronic Properties of Organic One-Dimensional Nanostructures. *Acc. Chem. Res.* **2010**, *43*, 409−418.

(2) Zheng, H.; Li, Y.; Liu, H.; Yin, X.; Li, Y. Construction of Heterostructure Materials toward Functionality. *Chem. Soc. Rev.* **2011**, *40*, 4506−4524.

(3) Grimsdale, A. C.; Müllen, K. The Chemistry of Organic Nanomaterials. *Angew. Chem., Int. Ed.* **2005**, *44*, 5592−5629.

(4) Palmer, L. C.; Stupp, S. I. Molecular Self-Assembly into One-Dimensional Nanostructures. *Acc. Chem. Res.* **2008**, *41*, 1674−1684.

(5) Xiao, J.; Yin, Z.; Li, H.; Zhang, Q.; Boey, F.; Zhang, H.; Zhang, Q. Postchemistry of Organic Particles: When TTF Microparticles Meet TCNQ Microstructures in Aqueous Solution. *J. Am. Chem. Soc.* **2010**, *132*, 6926−6928.

(6) Xiao, J.; Yin, Z.; Wu, Y.; Guo, J.; Cheng, Y.; Li, H.; Huang, Y.; Zhang, Q.; Ma, J.; Boey, F.; Zhang, H.; Zhang, Q. Chemical Reaction Between Ag Nanoparticles and TCNQ Microparticles in Aqueous Solution. *Small* **2011**, *7*, 1242−1246.

(7) Liu, H.; Xu, J.; Li, Y.; Li, Y. Aggregate Nanostructures of Organic Molecular Materials. *Acc. Chem. Res.* **2010**, *43*, 1496−1508.

(8) Hoeben, F. J. M.; Jonkheijm, P.; Meijer, E. W.; Schenning, A. P. H. J. About Supramolecular Assemblies of π-Conjugated Systems. *Chem. Rev.* **2005**, *105*, 1491−1546.
(9) Zang, L.; Che, Y.; Moore, J. F. One-Dimensional Self-Assembly of Planar π-Conjugated Molecules: Adaptable Building Blocks for Organic Nanodevices. *Acc. Chem. Res.* **2008**, *41*, 1596−1608.
(10) Li, G.; Wu, Y.; Gao, J.; Wang, C.; Li, J.; Zhang, H.; Zhao, Y.; Zhao, Y.; Zhang, Q. Synthesis and Physical Properties of Four Hexazapentacene Derivatives. *J. Am. Chem. Soc.* **2012**, *134*, 20298−20301.
(11) Yang, B.; Xiao, J.; Wong, J.; Guo, J.; Wu, Y.; Ong, L.; Lao, L.; Boey, F.; Zhang, H.; Yang, H.; Zhang, Q. Shape-Controlled Micro/Nanostructures of 9,10-Diphenylanthracene (DPA) and Their Application in Light-Emitting Devices. *J. Phys. Chem. C* **2011**, *115*, 7924−7927.
(12) Xiao, J.; Yin, Z.; Yang, B.; Liu, Y.; Ji, L.; Guo, J.; Huang, L.; Liu, X.; Yan, Q.; Zhang, H.; Zhang, Q. Preparation, Characterization, Physical Properties, and Photoconducting Behaviour of Anthracene Derivative Nanowires. *Nanoscale* **2011**, *3*, 4720−4723.
(13) Gianni, Z.; Barbara, V.; Anna, B. Monolayers and Multilayers of Conjugated Polymers as Nanosized Electronic Components. *Acc. Chem. Res.* **2008**, *41*, 1098−1109.
(14) Kivala, M.; Diederich, F. Acetylene-Derived Strong Organic Acceptors for Planar and Nonplanar Push−Pull Chromophores. *Acc. Chem. Res.* **2008**, *42*, 235−248.
(15) Cui, S.; Liu, H.; Gan, L.; Li, Y.; Zhu, D. Fabrication of Low-Dimension Nanostructures Based on Organic Conjugated Molecules. *Adv. Mater.* **2008**, *20*, 2918−2925.
(16) Liu, H.; Zhao, Q.; Li, Y.; Liu, Y.; Lu, F.; Zhuang, J.; Wang, S.; Jiang, L.; Zhu, D.; Yu, D.; Chi, L. Field Emission Properties of Large Area Nanowires of Organic Charge Transfer Complexes. *J. Am. Chem. Soc.* **2005**, *127*, 1120−1121.
(17) Cui, S.; Li, Y.; Guo, Y.; Liu, H.; Song, Y.; Xu, J.; Lv, J.; Zhu, M.; Zhu, D. Fabrication and Field Emission Properties of Large-Area Nanostructures of Organic Charge-Transfer Complex of Cu-TCNAQ. *Adv. Mater.* **2008**, *20*, 309−313.
(18) Ouyang, C.; Qian, X.; Wang, K.; Liu, H. Controllable One-Dimension Nanostructures of CuTNAP for Field Emission Properties. *Dalton Trans.* **2012**, *41*, 14391−14396.
(19) Yang, X.; Zhang, G.; Li, L.; Zhang, D.; Chi, L.; Zhu, D. Self-Assembly of a Dendron-Attached Tetrathiafulvalene: Gel Formation and Modulation in the Presence of Chloranil and Metal Ions. *Small* **2012**, *8*, 578−584.
(20) Zhang, X. J.; Zhang, X. H.; Shi, W.; Meng, X.; Lee, C.-S.; Lee, S.-T. Single-Crystal Organic Microtubes with a Rectangular Cross Section. *Angew. Chem., Int. Ed.* **2007**, *46*, 1525−1528.
(21) Jordan, B. J.; Ofir, Y.; Patra, D.; Caldwell, S. T.; Kennedy, A.; Joubanian, S.; Rabani, G.; Cooke, G.; Rotello, V. M. Controlled Self-Assembly of Organic Nanowires and Platelets Using Dipolar and Hydrogen-Bonding Interactions. *Small* **2008**, *4*, 2074−2078.
(22) Xu, J.; Liu, X.; Lv, J.; Zhu, M.; Huang, C.; Zhou, W.; Yin, X.; Liu, H.; Li, Y.; Ye, J. Morphology Transition and Aggregation-Induced Emission of an Intramolecular Charge-Transfer Compound. *Langmuir* **2008**, *24*, 4231−4237.
(23) Coropceanu, V.; Cornil, J.; Da Silva Filho, D. A.; Olivier, Y.; Silbey, R.; Brédas, J. L. Charge Transport in Organic Semiconductors. *Chem. Rev.* **2007**, *107*, 926−952.
(24) Brédas, J.; Beljonne, D.; Coropceanu, V.; Cornil, J. Charge-Transfer and Energy-Transfer Processes in π-Conjugated Oligomers and Polymers: A Molecular Picture. *Chem. Rev.* **2004**, *104*, 4971−5003.
(25) Grabowski, Z. R.; Rotkiewicz, K.; Rettig, W. Structural Changes Accompanying Intramolecular Electron Transfer: Focus on Twisted Intramolecular Charge-Transfer States and Structures. *Chem. Rev.* **2003**, *103*, 3899−4031.
(26) Myers, A. B. Resonance Raman Intensities and Charge-Transfer Reorganization Energies. *Chem. Rev.* **1996**, *96*, 911−926.
(27) Zyss, J.; Ledoux, I.; Volkov, S.; Chernyak, V.; Mukamel, S.; Bartholomew, G. P.; Bazan, G. C. Through-Space Charge Transfer and Nonlinear Optical Properties of Substituted Paracyclophane. *J. Am. Chem. Soc.* **2000**, *122*, 11956−11962.
(28) Lee, J. Y.; Kim, K. S.; Mhin, B. J. Intramolecular charge transfer of π-conjugated push−pull systems in terms of polarizability and electronegativity. *J. Chem. Phys.* **2001**, *115*, 9484−9489.
(29) Sachs, S. B.; Dubek, S. P.; Hsung, R. P.; Sita, L. R.; Smalley, J. F.; Newton, M. D.; Feldberg, S. W.; Chidsey, C. E. D. Rates of Interfacial Electron Transfer through π-Conjugated Spacers. *J. Am. Chem. Soc.* **1997**, *119*, 10563−10564.
(30) Li, Y.; Qing, Z.; Yu, Y.; Liu, T.; Jiang, R.; Li, Y. Synthesis and Self-Assembly of Dihydroxyperylene Bisimides for the Tuning of Photophysical Properties. *Chem.—Asian J.* **2012**, *7* (8), 1934−1939.
(31) Li, Y.; Xu, L.; Jiang, R.; Liu, H.; Li, Y. Synthesis of Amino-Substituted Pyrrole-Fused Perylenebis(dicarboximide) Derivatives by a One-Pot Azidation/Reduction/Cyclization. *Eur. J. Org. Chem.* **2013**, *31*, 7076−7082.
(32) Li, Y.; Xu, L.; Liu, T.; Yu, Y.; Liu, H.; Li, Y.; Zhu, D. Anthraceno-Perylene Bisimides: The Precursor of a New Acene. *Org. Lett.* **2011**, *13* (20), 5692−5695.
(33) Chen, S.; Li, Y.; Yang, W.; Chen, N.; Liu, H.; Li, Y. Synthesis and Tuning Optical Nonlinear Properties of Molecular Crystals of Benzothiadiazole Dyads. *J. Phys. Chem. C* **2010**, *114*, 15109−15115.
(34) Jiu, T.; Li, Y.; Liu, H.; Ye, J.; Liu, X.; Jiang, L.; Yuan, M.; Li, J.; Li, C.; Wang, S.; Zhu, D. Brightly full-color emissions of oligo(p-phenylenevinylene)s: substituent effects on photophysical properties. *Tetrahedron* **2007**, *63*, 3168−3172.
(35) Lv, J.; Yin, X.; Zheng, H.; Li, Y.; Li, Y.; Zhu, D. The configuration, solvatochromism and metallo-responses of two novel cyano-containing oligo(phenylene-vinylene) derivatives. *Luminescence* **2011**, *26* (3), 185−190.
(36) Chen, S.; Li, Y.; Liu, C.; Yang, W.; Li, Y. Strong Charge-transfer Chromophores by [2 + 2] Cycloaddition of TCNE and TCNQ to Periphery Donor-substituted Alkynes. *Eur. J. Org. Chem.* **2011**, 6445−6451.
(37) Xu, J.; Wen, L.; Zhou, W.; Lv, J.; Guo, Y.; Zhu, M.; Liu, H.; Li, Y.; Jiang, L. Asymmetric and Symmetric Dipole-Dipole Interactions Drive Distinct Aggregation and Emission Behavior of Intramolecular Charge-Transfer Molecules. *J. Phys. Chem. C* **2009**, *113*, 5924−5932.
(38) Liu, T.; Li, Y.; Yan, Y.; Li, Y.; Yu, Y.; Chen, N.; Chen, S.; Liu, C.; Zhao, Y.; Liu, H. Tuning Growth of Low-Dimensional Organic Nanostructures for Efficient Optical Waveguide Applications. *J. Phys. Chem. C* **2012**, *116*, 14134−14138.
(39) Yu, Y.; Li, Y.; Qin, Z.; Jiang, R.; Liu, H.; Li, Y. Designed synthesis and supramolecular architectures of furan-substituted perylene diimide. *J. Colloid Interface. Sci.* **2013**, *399*, 13−18.
(40) Chen, S.; Qin, Z.; Liu, T.; Wu, X.; Li, Y.; Liu, H.; Song, Y.; Li, Y. Aggregation-Induced Emission on Benzothiadiazole Dyads with Large Third-Order Optical Nonlinearity. *Phys. Chem. Chem. Phys.* **2013**, *15*, 12660−12666.
(41) Jiang, D.; Xue, Z.; Li, Y.; Liu, H.; Yang, W. Synthesis of Donor−Acceptor Molecules Based on Isoxazolones for Investigation of Their Nonlinear Optical Properties. *J. Mater. Chem. C* **2013**, *1*, 5694−5700.
(42) Xu, J.; Zheng, H.; Liu, H.; Zhou, C.; Zhao, Y.; Li, Y.; Li, Y. Crystal Hierarchical Supramolecular Architectures from 1-D Precursor Single-Crystal Seeds. *J. Phys. Chem. C* **2010**, *114*, 2925−2931.
(43) Chen, S.; Chen, N.; Yan, Y.; Liu, T.; Yu, Y.; Li, Y.; Liu, H.; Zhao, Y.; Li, Y. Controlling growth of molecular crystal aggregates for efficient optical Waveguides. *Chem. Commun.* **2012**, *48*, 9011−9013.
(44) Liu, T.; Yu, Y.; Chen, S.; Li, Y.; Liu, H. Self-assembly of a tripyrenylboron molecule towards solid sensor for fluoride anions. *RSC Adv.* **2013**, *3*, 9973−9977.
(45) Zhou, W.; Xu, J.; Zheng, H.; Yin, X.; Zuo, Z.; Liu, H.; Li, Y. Distinct Nanostructures from a Molecular Shuttle: Effects of Shuttling Movement on Nanostructural Morphologies. *Adv. Funct. Mater.* **2009**, *19*, 141−149.
(46) Nguyen, T.-Q.; Martel, R.; Bushey, M.; Avouris, P.; Carlsen, A.; Nuckolls, C.; Brus, L. Self-assembly of 1-D organic semiconductor nanostructures. *Phys. Chem. Chem. Phys.* **2007**, *9*, 1515−1532.

(47) Huang, C.; Li, Y.; Song, Y.; Li, Y.; Liu, H.; Zhu, D. Ordered Nanosphere Alignment of Porphyrin for Improvement in Nonlinear Optical Properties. *Adv. Mater.* **2010**, *22*, 3532−3536.
(48) Li, Z.; Liu, Y.; Kim, H.; Hales, J. M.; Jang, S.-H.; Luo, J.; Baehr-Jones, T.; Hochberg, M.; Marder, S. R.; Perry, J. W.; Jen, A. K. Y. High-Optical-Quality Blends of Anionic Polymethine Salts and Polycarbonate with Enhanced Third-Order Non-linearities for Silicon-Organic Hybrid Devices. *Adv. Mater.* **2012**, *24*, OP326−OP330.
(49) Eaton, D. F. Nonlinear Optical Materials. *Science* **1991**, *253*, 281−287.
(50) Xu, J.; Semin, S.; Niedzialek, D.; Kouwer, P. H. J.; Fron, E.; Coutino, E.; Savoini, M.; Li, Y.; Hofkens, J.; Uji-I, H.; Beljonne, D.; Rasing, T.; Rowan, A. E. Self-Assembled Organic Microfibers for Nonlinear Optics. *Adv. Mater.* **2013**, *25*, 2084−2089.
(51) Yu, Y.; Shi, Q.; Li, Y.; Liu, T.; Zhang, L.; Shuai, Z.; Li, Y. Solid Supramolecular Architecture of a Perylene Diimide Derivative for Fluorescent Enhancement. *Chem.—Asian J.* **2012**, *7*, 2904−2911.
(52) Yuan, M.; Li, Y.; Li, J.; Li, C.; Liu, X.; Lv, J.; Xu, J.; Liu, H.; Wang, S.; Zhu, D. A Colorimetric and Fluorometric Dual-modal Assay for Mercury Ion by a Molecule. *Org. Lett.* **2007**, *9*, 2313−2316.
(53) Zhu, M.; Yuan, M.; Liu, X.; Xu, J.; Lv, J.; Huang, C.; Liu, H.; Li, Y.; Wang, S.; Zhu, D. Visible Near-Infrared Chemosensor for Mercury Ion. *Org. Lett.* **2008**, *10*, 1481−1484.
(54) Xu, L.; Li, Y.; Yu, Y.; Liu, T.; Cheng, S.; Liu, H.; Li, Y. A Receptor Incorporating OH, NH and CH Binding Motifs for a Fluoride Selective Chemosensor. *Org. Biomol. Chem.* **2012**, *10*, 4375−4380.